TRANSPORT IN TWO-DIMENSIONAL QUANTUM WELL HEMTS

John P. Kreskovsky* and H.L. Grubin*
Scientific Research Associates, Inc.
50 Nye Road, P.O. Box 1058
Glastonbury, CT 06033-6058

Abstract

A parametric study of quantum well HEMT structure is performed through numerical simulations based on a set of quantum hydrodynamics equations. From a reference structure, the effects of variations in planar layer doping, gate recess depth and channel depth on device performance are investigated. The role of the quantum potential in establishing the 2-DEG in the channel is also examined.

I. Introduction

Advances in modeling and computational techniques have now made it possible to simulate and study relatively complex devices on a highly sophisticated level. In this paper we apply a set of quantum hydrodynamic equations to the simulation of an advanced quantum well HEMT to further gain an understanding of the detailed transport within such structures and to demonstrate how such a simulation can be used to obtain quantitative information on how variations of relevant design parameters affect device performance. We begin with the reference structure shown in Fig. 1, an InP-based HEMT with an 800 angstrom InGaAs channel on an AlInAs buffer layer. A 200 angstrom AlInAs Schottky enhancement layer separates the channel from the N^+ InGaAs cap layer, and a 30 angstrom spacer layer separates the channel from the Si doped planar layer. The gate is recessed 100 angstroms into the enhancement layer. Such structures have been the focus of much recent attention; e.g., Refs. [1-3]. The role of quantum mechanics in the analysis of such structures is readily apparent in that the channel is a quantum well in which a 2-DEG gas forms at the interface between the channel and the spacer layer. This 2-DEG is seeded by the planar doped layer.

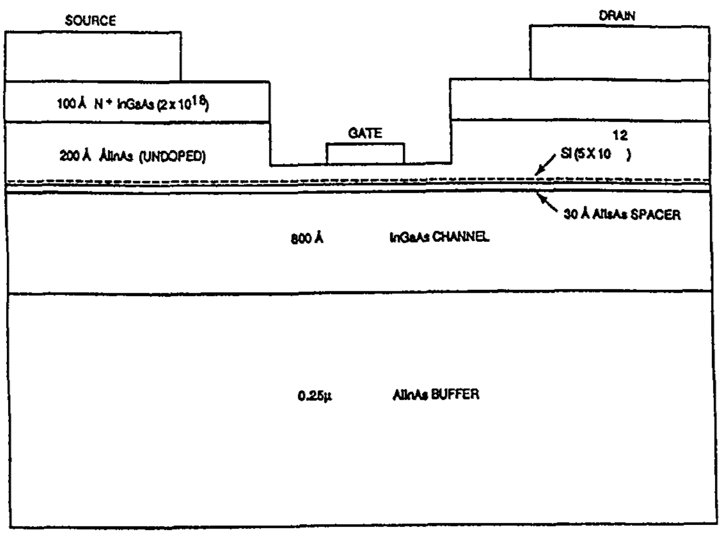

Figure 1. Quantum well HEMT structure used in one and two dimensional simulations.

The equations implemented in our simulation procedure are the hydrodynamics transport equations with corrections for quantum mechanical effects. Various formulations of these equations have appeared in the literature [4].

*Supported in part by ARO and ONR

II. Simulated Results

To begin our simulations we compute the equilibrium solution at zero bias to establish the 2-DEG in the channel. We compare the distribution of electrons in the channel with the classical result in Fig. 2. Figure 2a shows the result under the cap layer and 2b shows the result under the gate. We note that the quantum effects reduce the peak and raise the minimum densities at the heterojunction and yield a continuous density variation. It is also of interest to examine the quantum potential in the region surrounding the gate. Figure 3 shows a blow-up of the quantum potential under equilibrium conditions. The region extends only partly into the channel. The most significant feature here is that the quantum potential shows a nearly one-dimensional structure in the direction normal to the heterojunction interfaces, even at the edge of the gate recess. Some two-dimensionality is observed at the edge of the gate, at the gate surface, but in the channel the structure is still primarily one-dimensional in spite of the depletion of the 2-DEG. This is because the gradients of the density normal to the heterojunction are much greater than those associated with the gate depletion region. The quantum potential thus plays its major role in establishing the structure of the 2-DEG profile normal to the interfaces.

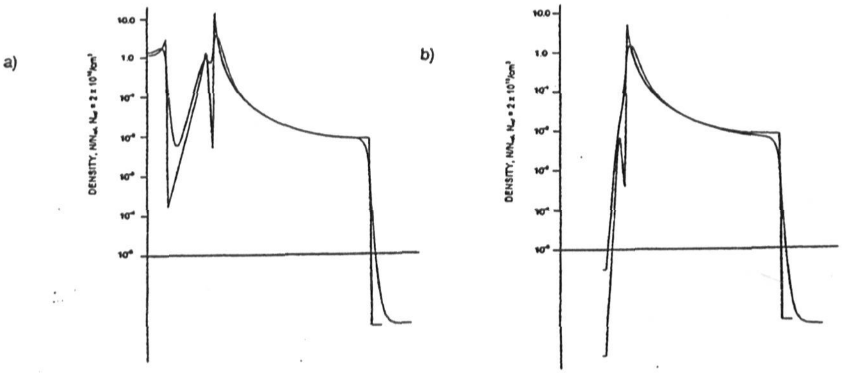

Figure 2. Comparison of classical and quantum corrected density distributions in a a plane normal to the device surface, a) under cap layer, b) under gate.

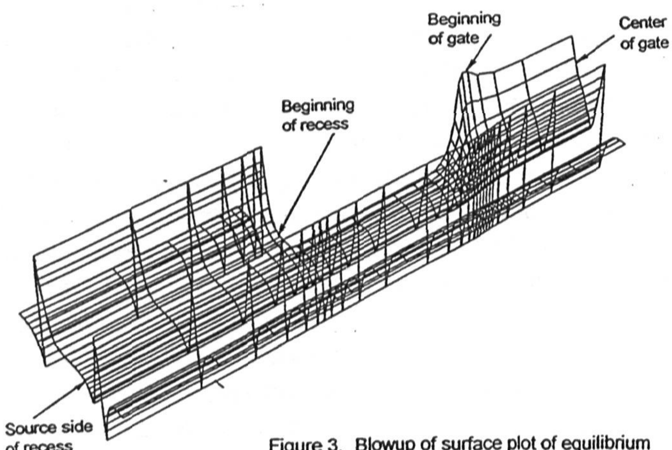

Figure 3. Blowup of surface plot of equilibrium quantum potential in region between the center of the gate contact and to the source side of the gate recess.

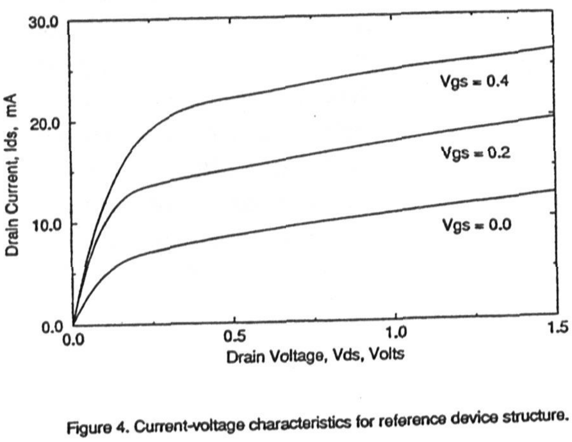

Figure 4. Current-voltage characteristics for reference device structure.

Figure 4 shows the predicted current voltage characteristics for the reference structure and Figure 5 shows surface plots of density, potential, velocity and temperature at a bias of $V_{ds} = 0.5$ volts and $V_{gs} = 0.4$ volts. The high concentration of electrons under the source and drain contacts was introduced to mimic the metalization of the contacts. We also not that the density, potential and velocity in the 2-DEG are almost constant except directly

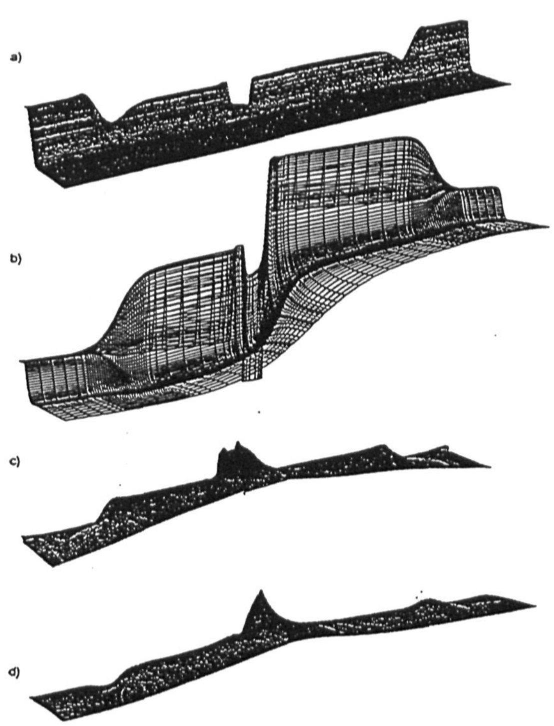

Figure 5. Surface plots of a) density, b) potential, c) velocity and d) temperature at V_{ds} = 0.5, V_{gs} = 0.4 volts.

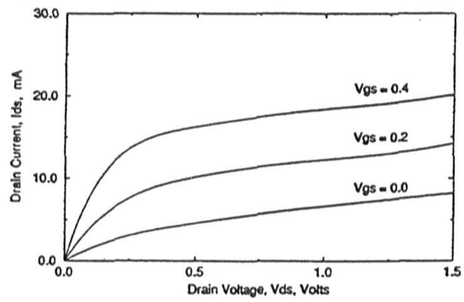

Figure 6. Current-voltage characteristics for a 20% reduction in planar layer doping.

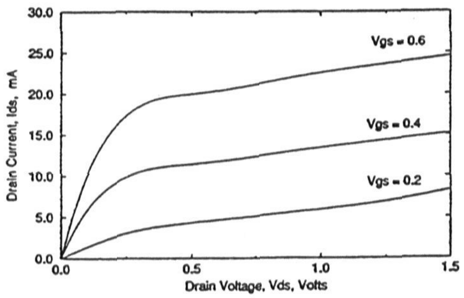

Figure 7. Current-voltage characteristics for a gate recess increased from 100 to 150 angstroms.

under the gate. Under the gate the velocity approaches 1.35 x 10^7 cm/sec. There is also some heating of the electrons; however, this is surprisingly small. The peak temperature at this bias reaches only 340°K. For this structure we obtained a transconductance of 705 ms/mm, a capacitance of 0.0387 pf and a cutoff frequency of 144.7 GHz at V_{ds} = 1.0 volts and V_{gs} = 0.2 volts. The transconductance was nearly constant over the gate bias investigated while f_τ varied from 156 GHz at V_{gs} = 0.0 to 135 GHz at V_{gs} = 0.4.

Having established the performance and characteristics of the reference structure we then began our parametric study by reducing the doping of the planar layer. The I-V characteristics for this structure are shown in Fig. 6. The results show a reduction in the current level due to the reduced conductivity of the channel. The saturation characteristics of this device are also slightly harder indicating higher output resistance. The transconductance, capacitance and cutoff frequency for this structure were found to be 587 ms/mm, 0.035 pf and 135.5 GHz, respectively at V_{ds} = 1.0 volts and V_{gs} = 0.2 volts. The transconductance varied from 530 ms/mm to 640 ms/mm, while f_τ ranged from 138 GHz to 131 GHz.

We next increased the gate recess depth to 150 Å. This would be expected to reduce the current levels since the closer proximity of the gate to the channel would result in greater depletion at a given bias level. We would also expect an increase in the transconductance and capacitance. Figure 7 shows that this is indeed the case. The current levels are significantly lower than the reference structure. A bias of 0.6 volts on the gate is required to obtain current levels previously obtained at V_{gs} = 0.4 volts. At V_{gs} = 0.2 volts and V_{ds} = 1.0 volts the transconductance, capacitance and cutoff frequency are virtually the same as the original structure. However, when we compared the results based on the drain current level we found that this structure did exhibit higher tranconductance and capacitance, but the cutoff frequency remained in the range of 145 GHz. At V_{gs} = 0.4 volts g_m was approximately 850 ms/ms and the capacitance about 0.45 pf. This structure also showed significantly greater variation in transconductance and capacitance with gate bias than the other structure.

The final simulations were performed for a device in which the channel depth was reduced to 200 angstroms.

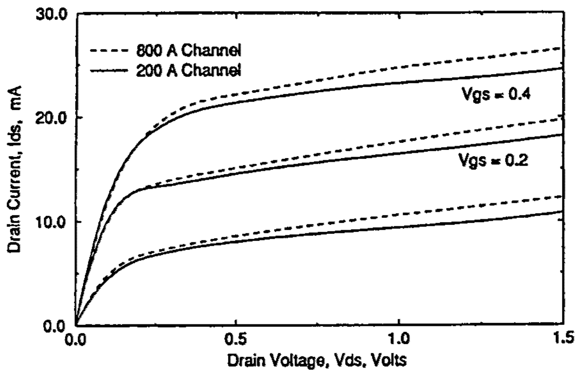

Figure 8. Current-voltage characteristics for a reduction in channel depth from 800 to 200 angstroms.

The current-voltage characteristics for this structure are shown in Fig. 8, where they are compared to the reference structure. The reduced channel depth results in greater confinement and harder saturation. This difference in the output conductance is further reflected in the transconductance, capacitance and cutoff frequency. At $V_{gs} = 0.2$ and $V_{ds} = 1.0$ these quantities were 680 ms/mm, 0.037 pf and 147 GHz. Another interesting result for this structure was that the transconductance decreased with increasing gate bias, from 737 ms/mm at $V_{gs} = 0.0$ to 625 ms/mm at $V_{gs} = 0.4$. In all the other devices the transconductance increased with increasing gate bias. The result was such that at low gate bias the cutoff frequency exceeded 190 GHz but at high gate bias it dropped to a low of 111 GHz. Thus, this device exhibited the highest and lowest cutoff frequencies of any of the devices investigated, depending on the bias level.

III. Conclusions

We have applied a set of quantum corrected hydrodynamic equations to investigate transport in quantum-well HEMTs. The results of the study show the importance of the quantum potential in establishing the distribution of charge in the 2-DEG in the channel. Surprisingly the results also show that quantum effects predominantly influence the density distribution normal to the heterojunction interfaces. The role of the quantum potential in affecting transport in the 2-DEG along the channel, even under the gate, appears limited. This is because the gradients in the density normal to the interfaces are much greater than those along the channel, including channel-wise gradients at the edges of the depletion region. However, the quantum mechanical corrections must be included if the distribution of charge and the charge sheet density of the 2-DEG is to be accurately predicted.

We have also applied our simulation procedure to study the effect of various device design parameters on device performance. In this way we have demonstrated the usefulness of such a procedure in both initial device design and optimization of a device.

IV. References

1) V. Zhao, D.C. Tsui, and P.C. Chao, "Electron Transport in 0.15-µm Gate $In_{0.52}Al_{0.48}As/In_{0.53}Ga_{0.47}As$ HEMT," *IEEE Trans. Electron Devices*, vol. 40, no. 6, pp. 1067-1070, June 1993.

2) L.D. Nguyen, A. S. Brown, M.A. Thompson and L.M. Jelloian, "50-nm Self-Aligned-Gate Pseudomorphic AlInAs/GaInAs High Electron Mobility Transistors," *IEEE Trans. Electron Devices*, vol. 39, no. 9, pp. 2007-2014, Sept. 1992.

3) R. Plana, L. Escotte, O. Llopis, H. Amine, T. Parra, M. Gayral, and J. Graffeuil, "Noise in AlGaAs/InGaAs/GaAs Pseudomorphic HEMTs from 10 Hz to 18 GHz," *IEEE Trans. Electron Devices*, vol. 40, no. 5, pp. 852-858, May 1993.

4) H.L. Grubin and J.P. Kreskovsky, "Quantum Moment Balance Equations and Resonant Tunneling Structures," *Solid State Electronics*, vol. 32, no. 12, pp. 1071, 1075, 1989.